NASA TECHNICAL NOTE

NASA TN D-4817

NASA TN D-4817

A STUDY OF THE REACTION-PLANE APPROXIMATION IN ABLATION ANALYSES

by C. W. Stroud

Langley Research Center
Langley Station, Hampton, Va.

NATIONAL AERONAUTICS AND SPACE ADMINISTRATION • WASHINGTON, D. C. • OCTOBER 1968

A STUDY OF THE REACTION-PLANE APPROXIMATION IN ABLATION ANALYSES

By C. W. Stroud

Langley Research Center
Langley Station, Hampton, Va.

NATIONAL AERONAUTICS AND SPACE ADMINISTRATION

For sale by the Clearinghouse for Federal Scientific and Technical Information
Springfield, Virginia 22151 – CFSTI price $3.00

A STUDY OF THE REACTION-PLANE APPROXIMATION IN ABLATION ANALYSES*

By C. W. Stroud
Langley Research Center

SUMMARY

Equations which describe the reactive zone in charring ablators during steady-state ablation are derived. Average reaction-zone temperatures and reaction-zone thicknesses are studied for half-order, first-order, and second-order reactions. This study was made for each of these reaction orders over a wide range of frequency factors and heats of pyrolysis. One technique used to simplify ablation analyses is to idealize the degradation process and assume that it occurs in a plane. The purpose of this paper is to investigate the validity of this technique as a good engineering approximation. Empirical relations are developed between the frequency factors and the average reaction-zone temperature for the three reaction orders. These relations are used to locate the reaction zone in a reaction-plane analysis. The resulting temperature profile is shown to be in substantial agreement with the profile obtained from a reaction-in-depth analysis.

INTRODUCTION

Ablative materials are used to protect spacecraft from the thermal environment encountered when entering planetary atmospheres. Char-forming ablators provide the most effective thermal protection for a range of entry environments. The excellent performance of these char-forming materials results from a number of complex thermal, chemical, and mass-transfer processes. A number of numerical analyses covering the complex processes have been conducted and programed for computer solution. (See refs. 1 and 2, for example.) These analyses take into account many important parameters.

Studies of the processes that occur in the zone where ablation materials decompose to yield char and gaseous products are reported in references 3 and 4. Assumptions were made in each of these analyses which had the effect of uncoupling the mass and energy equations.

*Some of the material in this paper was included in a thesis entitled "A Study of the Chemical Reaction Zone in Charring Ablators During Thermal Degradation" submitted in partial fulfillment of the requirements for the degree of Master of Science in Engineering Mechanics, Virginia Polytechnic Institute, September 1965.

One of the techniques used to simplify ablation analyses is to idealize the degradation process and assume that it occurs in a plane. The purpose of the present paper is to investigate the validity of this technique as a good engineering approximation. This paper presents the results of a simplified quasi-steady-state analysis of the processes that occur in the reaction zone of a charring ablator when the mass and energy equations are coupled. The effects of thermal, chemical, and ablative characteristics of the material are investigated in terms of temperature and density profiles. The physical dimensions of the decomposition zone are given. The proper placement of the reaction-plane interface is investigated and a simplified method for incorporating the effects of pyrolysis reactions in more general analyses is discussed.

SYMBOLS

The units used in the physical quantities defined in this section are given in the International System of Units (SI). (See ref. 5.)

A frequency factor, s^{-1}

$\overline{A}$ dimensionless frequency factor, $\frac{kA}{\rho_o c_p v^2}$

c_p specific heat of solid, joules/kilogram-degree Kelvin

$c_{p,g}$ specific heat of gas, joules/kilogram-degree Kelvin

d thermocouple depth, meters

ΔE activation energy, joules/mole

H total enthalpy, joules/kilogram

ΔH heat of pyrolysis, joules/kilogram

$\overline{\Delta H}$ dimensionless heat of pyrolysis, $\frac{\Delta H R \rho_{i,o}}{\Delta E c_p \rho_o}$

h enthalpy, joules/kilogram

h_e enthalpy external to boundary layer, joules/kilogram (figs. 9 and 10)

k thermal conductivity, watts/meter-degree Kelvin

$\dot{m}$	mass-flow rate, kilograms/meter^2-second
N	number of reacting species
n	reaction order
$\dot{q}_{cw}$	cold-wall convective heating rate (figs. 9 and 10)
R	universal gas constant, 8.3143 joules/mole-degree Kelvin
T	temperature, degrees Kelvin
v	surface-recession rate, meters/second
y	coordinate normal to surface, meters
η	dimensionless coordinate normal to surface, $\xi \frac{c_p v \rho_o}{k}$
θ	dimensionless temperature, $\frac{RT}{\Delta E}$
ξ	coordinate defined by the transformation, $y - v\tau$, meters
ρ	density, kilograms/meter^3
$\overline{\rho}_i$	dimensionless density, $\frac{\rho_i}{\rho_{i,o}}$
τ	time, seconds

Subscripts:

c	char
g	gas
i	integer denoting ith species
m	median
o	initial

ANALYSIS

The mechanism of ablation in charring ablators is complex. It is mathematically described by a set of nonlinear partial differential equations. (See ref. 1, for example.) The purpose of this paper is not to attempt the solution of the complete problem but to focus attention on describing the reaction zone of a charring ablator such as the one in figure 1. In order to eliminate the transient effects caused by a change in the external environment, an assumption of steady-state ablation is made. This assumption reduces the equations to nonlinear ordinary differential equations. The equations are then put in a form which can be solved numerically to yield the steady-state temperature and density profiles. Thus, attention is centered on the properties of the reaction zone such as thickness and median temperature. After all quantities are put in dimensionless form, the problem is studied by specifying two parameters, frequency factor and heat of pyrolysis, for each reaction. The frequency factor is characterized in simple bimolecular reactions as the frequency of collisions of the reacting molecules. For pyrolysis reactions, the frequency factor may be interpreted as an entropy of activation. The heat of pyrolysis characterizes the net amount of energy involved in the pyrolysis reactions. Once these parameters are specified, the equations are solved numerically for the density and temperature as a function of location within the ablator.

The energy flow is approximately one dimensional through a large blunt body entering an atmosphere or through an ablative coating of a rocket nozzle exposed to exhaust gases. Therefore, the energy equation for a chemically reacting solid can be approximated (ref. 6) by

$$\frac{\partial}{\partial \tau}\left(\sum_{i=1}^{N} \rho_i H_i\right) = \frac{\partial}{\partial y}\left(k \frac{\partial T}{\partial y} + \sum_{i=1}^{N} \dot{m}_{g,i} H_{g,i}\right) \tag{1}$$

where the summation is carried out over the number of reacting species making up the ablation material. This equation can be expanded to give

$$\sum_{i=1}^{N}\left(\frac{\partial \rho_i}{\partial \tau} H_i + \frac{\partial H_i}{\partial \tau} \rho_i - \frac{\partial \dot{m}_{g,i}}{\partial y} H_{g,i} - \frac{\partial H_{g,i}}{\partial y} \dot{m}_{g,i}\right) = \frac{\partial}{\partial y}\left(k \frac{\partial T}{\partial y}\right) \tag{2}$$

The kinetic energy of the transpiring gases is typically three orders of magnitude less than the chemical and thermal energy terms and is, therefore, neglected. With this assumption, the total energy is equal to the enthalpy. The pressure is assumed to remain constant throughout the material. This assumption is reasonable where an assumption of

one-dimensional heat flow is appropriate. With these two assumptions, equation (2) can be put in the form

$$\sum_{i=1}^{N}\left(\frac{\partial \rho_i}{\partial \tau} h_i + \rho_i c_{p,i} \frac{\partial T}{\partial \tau} - \frac{\partial \dot{m}_{g,i}}{\partial y} h_{g,i} - \dot{m}_{g,i} c_{p,g,i} \frac{\partial T}{\partial y}\right) = \frac{\partial}{\partial y}\left(k \frac{\partial T}{\partial y}\right) \tag{3}$$

From the continuity equation for one-dimensional mass flow, the following equation is obtained:

$$\frac{\partial \rho_i}{\partial \tau} = \frac{\partial \dot{m}_{g,i}}{\partial y} \tag{4}$$

Substitution of equation (4) into equation (3) yields

$$\sum_{i=1}^{N} \rho_i c_{p,i} \frac{\partial T}{\partial \tau} = \frac{\partial}{\partial y}\left(k \frac{\partial T}{\partial y}\right) + \sum_{i=1}^{N}\left[\frac{\partial \rho_i}{\partial \tau}\left(h_{g,i} - h_i\right) + \dot{m}_{g,i} c_{p,g,i} \frac{\partial T}{\partial y}\right] \tag{5}$$

The coordinate ξ is defined by the transformation

$$\xi = y - v\tau \tag{6}$$

If it is assumed that a quasi-steady state exists and that v and k are constant, equation (5) can be put in the following form:

$$k \frac{d^2T}{d\xi^2} + \sum_{i=1}^{N}\left(c_{p,g,i} \dot{m}_{g,i} \frac{dT}{d\xi} - v \Delta H_i \frac{d\rho_i}{d\xi} + v \rho_i c_{p,i} \frac{dT}{d\xi}\right) = 0 \tag{7}$$

By assuming that the specific heats of all constituents are the same and by noting that for a quasi-steady-state solution the total mass flow is constant and can be written

$$\dot{m}_g = v\rho_o - v \sum_{i=1}^{N} \rho_i \tag{8}$$

equation (7) becomes

$$k \frac{d^2T}{d\xi^2} + \sum_{i=1}^{N} - v \Delta H_i \frac{d\rho_i}{d\xi} + \rho_o v c_p \frac{dT}{d\xi} = 0 \tag{9}$$

Integrating once and evaluating the constant of integration as $\xi \to \infty$ yields

$$k \frac{dT}{d\xi} + v \sum_{i=1}^{N} \Delta H_i\left(\rho_{i,o} - \rho_i\right) + c_p v \rho_o\left(T - T_o\right) = 0 \tag{10}$$

If the transformation

$$\eta = \xi \frac{c_p v \rho_o}{k} \tag{11}$$

is made, equation (10) becomes

$$\frac{dT}{d\eta} + \sum_{i=1}^{N} \left[\frac{\Delta H_i \rho_{i,o}}{c_p \rho_o} \left(1 - \frac{\rho_i}{\rho_{i,o}} \right) \right] + T - T_o = 0 \tag{12}$$

It is necessary to determine ρ_i as a function of T and η. This can be accomplished by considering the reaction equation based on the Arrhenius reaction-rate relation

$$\frac{d\bar{\rho}_i}{d\tau} = -\bar{\rho}_i^n A_i e^{-\frac{\Delta E_i}{RT}} \tag{13}$$

where A_i is the frequency factor and n is the order of the reaction.

Then, by using

$$\frac{d\bar{\rho}_i}{d\tau} = -v \frac{d\bar{\rho}_i}{d\xi} = -\frac{c_p \rho_o v^2}{k} \frac{d\bar{\rho}_i}{d\eta} \tag{14}$$

the following equation is obtained:

$$\frac{d\bar{\rho}_i}{d\eta} = \frac{k}{c_p \rho_o v^2} \bar{\rho}_i^n A_i e^{-\frac{\Delta E_i}{RT}} \tag{15}$$

For a reaction of order n

$$\int_1^{\bar{\rho}_i} \frac{d\bar{\rho}_i}{\bar{\rho}_i^n} = \frac{k}{c_p \rho_o v^2} A_i \int_0^{\eta} e^{-\frac{\Delta E_i}{RT}} d\eta + C \tag{16}$$

where C is the constant of integration. Integrating equation (16) and evaluating the constant as $\eta \to \infty$ gives, when $n \neq 1$

$$\bar{\rho}_i = \left[(n-1) \frac{k}{c_p \rho_o v^2} A_i \int_{\eta}^{\infty} e^{-\frac{\Delta E_i}{RT}} d\eta + 1 \right]^{\frac{1}{1-n}} \tag{17}$$

Integrating equation (16), when $n = 1$, yields

$$\bar{\rho}_i = \exp\left(\frac{-k}{c_p \rho_o v^2} A_i \int_{\eta}^{\infty} e^{-\frac{\Delta E_i}{RT}} d\eta \right) \tag{18}$$

When only one reaction is present, it is convenient to make the following transformation:

$$\theta = \frac{RT}{\Delta E} \tag{19}$$

Applying this transformation to equation (12),

$$\frac{d\theta}{d\eta} + \frac{R\,\Delta H\rho_{1,o}}{\Delta E c_p \rho_o}(1 - \bar{\rho}) + \theta - \frac{T_o R}{\Delta E} = 0 \tag{20}$$

where $\rho_{1,o}$ is the initial density of the one reactable species present.

Equation (17) or (18) and equation (20) were solved simultaneously by numerical methods to determine their value as a function of location in the ablation material. The numerical technique that was used consisted of first holding the value of temperature constant in the density equation and integrating the appropriate equation for density over a small spatial increment. Then, the density was held constant at its calculated value in equation (20) while this differential equation was solved over the same small spatial increment. This process was repeated in a step-by-step manner. The first-order differential equation for temperature was solved by using Adams' method (ref. 7, for example). Trapezoidal integration was used in the density equation. In order to determine the accuracy of this technique, comparisons were made with exact solutions. The exact solutions can be obtained when the heat of pyrolysis is zero and the density and temperature equations are thus uncoupled. The numerical and the exact solutions agreed to five decimal places. This degree of accuracy is more than adequate for this simplified analysis.

RESULTS AND DISCUSSION

Density Profiles

Figure 2 shows a plot of the local density through the reaction zone for two different values of frequency factor. The profiles shown are for first-order reactions (n = 1). The curves have been arbitrarily translated so that they coincide when 50 percent of the reactable material has decomposed. A reaction plane, which represents one approximation to the density profile, is also shown. For the quasi-steady-state condition, under consideration here, the char thickness is determined by the process by which char is removed at the surface. The char reaches an equilibrium thickness such that the linear velocity of the reaction zone is equal to the surface-recession rate. Therefore, the surface is located at some point to the left of the reaction zone shown in figure 2. This location depends on the environmental conditions.

The thickness of the reaction zone is defined as the distance between the point at which the local density reaches a value of 98 percent and the point at which it reaches a density of 2 percent of the original density of the reactable species. In the example shown, 80 percent of the original material is reactable. Figure 2 shows two frequency factors that are typical for a number of ablation materials. The reaction-zone thickness increases as the frequency factor decreases. With a frequency factor of 10^8 s^{-1}, the

reaction-zone thickness is 3.1 mm. With a frequency factor of 10^{12} s^{-1}, the reaction-zone thickness is 1.6 mm. This latter value is very small in terms of measurement capabilities, when the problems involved in determining the boundaries of the zone are considered. The effect of reaction-zone thickness on other aspects of performance must be determined from examination of temperature profiles.

Temperature Distributions

Typical temperature profiles are shown in figure 3. In these profiles, it was assumed that external conditions are such that a 2000° K surface temperature is reached and the surface-recession rate is the same for each curve. With zero heat of pyrolysis, the temperature distribution is independent of the kinetic constants, and the temperature is much higher at a given distance from the surface than with a large heat of pyrolysis.

The heat of pyrolysis used for the two lower curves is in the upper range of values that can be obtained with available materials. The decomposition reactions occur at the knee of the temperature curves. The reactions account for the higher rate of change in temperature at that point in each profile. At temperatures lower than the point where the reactions occur, the temperature at a given distance from the surface is lower for higher frequency factors. At higher temperatures where the decomposition reaction is complete, the temperature depends on the heat of pyrolysis and is independent of frequency factor. For the assumptions used here, the temperature is an exponential function of distance at all points except in the zone where decomposition occurs. The lower temperatures which are obtained at greater depths result from earlier completion of the reaction and hence earlier transition of the temperature to the exponential region after the reaction is completed; thus, the pyrolysis temperature is lowered.

Reaction-Zone Thickness

Figure 4 illustrates the effect of surface-recession rate on the reaction-zone thickness for two values of heat of pyrolysis. The calculations shown are for first-order reactions and a frequency factor of 10^{12} s^{-1}. The midrange velocity of 25 μm/s is a typical surface-recession rate obtained for a charring ablator. (See ref. 8, for example.) Increasing the surface-recession rate by a factor of 10 causes the reaction zone to become very thin. Decreasing the surface-recession rate by a factor of 10 causes the reaction zone to become thick enough to be significant when compared with the thickness of a typical ablator. When the ablation velocity is decreased, the classification of the ablation material as two layers with an interface between appears to be inadequate. The tendency is for an increase in the heat of pyrolysis to decrease the thickness of the reaction zone, but this decrease is not large. In general, higher values of the frequency factor result in thinner reaction zones. These trends are also found with reactions of other orders.

The effect of activation energy on reaction-zone thickness is shown in figure 5. The reaction-zone thickness is seen to be essentially independent of activation energy. This result might be expected after examination of equation (16). In that equation, the density is a function of activation energy only in terms of the ratio of activation energy to temperature. Therefore, it is anticipated that whereas the reaction-zone thickness is independent of activation energy, the pyrolysis temperature will be directly proportional to activation energy.

These results lead to an important conclusion regarding the effects of the frequency factor on ablative performance. The thickness of the reaction zone is controlled almost entirely by the frequency factor, whereas the pyrolysis temperature is strongly influenced by activation energy. Activation energy and frequency factor affect pyrolysis in different ways, hence a unique value of each must be determined if accurate results are required.

Median Temperature

The median temperature of reaction is defined herein as that temperature at which 50 percent of the reactable material has been degraded. The reaction-zone median temperature $\left(\frac{\Delta E}{RT}\right)_m$ is plotted in figure 6 as a function of dimensionless frequency factor for two values of heat of pyrolysis. This figure shows a linear relationship between the median temperature and the logarithm of the dimensionless frequency factor for the three reaction orders.

These results can be summarized in three equations. The median temperature $\frac{1}{\theta_m}$ is given for the half-order reaction by

$$\frac{1}{\theta_m} = -0.7 + 0.955 \ln \overline{A} - 2.2 \overline{\Delta H} \tag{21}$$

for the first-order reaction by

$$\frac{1}{\theta_m} = -1.50 + 0.955 \ln \overline{A} - 3.6 \overline{\Delta H} \tag{22}$$

and for the second-order reaction by

$$\frac{1}{\theta_m} = -1.70 + 0.945 \ln \overline{A} - 1.8 \overline{\Delta H} \tag{23}$$

when

$$\left.\begin{aligned} 0 \leqq \overline{\Delta H} \leqq 0.5 \\ 10^6 \leqq \overline{A} \leqq 10^{15} \end{aligned}\right\} \tag{24}$$

Equations (21), (22), and (23) can be solved for velocity. Thus, by use of equation (8), the mass-flow rate is, for half-order reactions

$$\dot{m}_{1/2} = (\rho_o - \rho_c)\sqrt{\frac{kA}{\rho_o c_p}}\, e^{-\frac{0.7+2.2\overline{\Delta H}}{2(0.955)}}\, e^{-\frac{1}{2(0.955\theta_m)}} \tag{25}$$

for first-order reactions

$$\dot{m}_1 = (\rho_o - \rho_c)\sqrt{\frac{kA}{\rho_o c_p}}\, e^{-\frac{1.5+3.6\overline{\Delta H}}{2(0.955)}}\, e^{-\frac{1}{2(0.955\theta_m)}} \tag{26}$$

and for second-order reactions

$$\dot{m}_2 = (\rho_o - \rho_c)\sqrt{\frac{kA}{\rho_o c_p}}\, e^{-\frac{1.7+1.8\overline{\Delta H}}{2(0.945)}}\, e^{-\frac{1}{2(0.945\theta_m)}} \tag{27}$$

The mass-flow rates determined from equations (25), (26), and (27) are the rates of pyrolysis of reaction-plane approximations. These flow rates locate the reaction plane at the median point in the reaction zone as shown in figure 2. Thus, the rate of pyrolysis is determined as a function of thermophysical properties and readily obtainable data from thermogravimetric analyses. The use of an equivalent reaction plane is thus placed on a rational basis. This correlation is only valid for one reactable species; hence, the summation signs do not appear in equations (25), (26), and (27). These equations for rate of pyrolysis can be inserted directly into other ablation analyses which utilize a reaction-plane approximation when one major pyrolysis reaction exists.

Reaction-Plane Approximation

With the information available on the rate of pyrolysis in equations (25), (26), and (27), comparison of the temperature distribution obtained from reaction-in-depth calculations with the distribution obtained from these equations is possible. The two lower curves in figure 3 (reactions in depth) are plotted in figure 7 with the corresponding curves calculated from equation (26) (reaction-plane approximation). For each frequency factor, the temperature distribution obtained with the reaction-plane approximation is close to that obtained with reactions in depth and nowhere do they differ more than a few degrees. This agreement indicates the accuracy that is possible when quasi-steady-state conditions exist.

The three equations for pyrolysis rate have been used in the transient ablation program described in reference 1. The calculated temperature histories of points inside ablation materials agree well with those measured by properly installed thermocouples even under transient conditions. Reference 9 is one well-documented example of the agreement that can be obtained by using the reaction-plane approximation. This

reference describes an extensive ground-test program that was conducted in support of a flight project. The model used in these ground tests is shown in figure 8. The results of eight tests are summarized in figure 9. The calculations accurately predict the measured recession of both the surface and the pyrolysis interface (reaction zone). As would be expected from the results of figure 7, when the reaction plane is correctly placed, the temperatures are accurately calculated. The calculated and measured temperatures of various points in two models are shown in figure 10. The agreement is remarkable even during the highly transient cool-down period documented by the thermocouple at a depth of 1.29 cm. Apparently the reaction-plane approximation provides a good engineering approximation to the actual temperature distribution even when conditions depart from the steady state. This agreement indicates that if the proper pyrolysis temperature is chosen, results can be obtained with a reaction plane which are comparable to those from the more complicated reaction-in-depth analyses.

CONCLUSIONS

Equations have been derived to study the reaction-zone thickness of ablation materials when significant heat of pyrolysis exists and the change in density across the reaction zone is considered. This technique has the effect of coupling the mass and energy equations. These equations were solved numerically for a wide range of quasi-steady-state conditions.

As a result of the study, the following conclusions are reached:

1. The temperature distribution through an ablation material depends strongly on the heat of pyrolysis.

2. Activation energy and frequency factor affect pyrolysis in different ways, hence a unique value of each must be determined if accurate results are required.

3. The total mass rate of pyrolysis and the median temperature of pyrolysis can be correlated on the basis of an Arrhenius function.

4. A reaction-plane analysis incorporating the Arrhenius pyrolysis-temperature function gives temperatures which are in satisfactory agreement with reaction-in-depth analyses and with experiment.

Langley Research Center,
National Aeronautics and Space Administration,
Langley Station, Hampton, Va., June 12, 1968,
124-08-03-26-23.

REFERENCES

1. Swann, Robert T.; Pittman, Claud M.; and Smith, James C.: One-Dimensional Numerical Analysis of the Transient Response of Thermal Protection Systems. NASA TN D-2976, 1965.

2. Munson, Thomas R.; and Spindler, Robert J.: Transient Thermal Behavior of Decomposing Materials. Part I – General Theory and Application to Convective Heating. RAD-TR-61-10 (Contracts AF04(647)-258 and -305), AVCO Corp., May 3, 1961.

3. Beecher, Norman; and Rosensweig, Ronald E.: Ablation Mechanisms in Plastics With Inorganic Reinforcement. ARS J., vol. 31, no. 4, Apr. 1961, pp. 532-539.

4. Kauzlarich, J. J.: Ablation of Reinforced Plastic for Heat Protection. Trans. ASME, Ser. E: J. Appl. Mech., vol. 32, no. 1, Mar. 1965, pp. 177-182.

5. Mechtly, E. A.: The International System of Units – Physical Constants and Conversion Factors. NASA SP-7012, 1964.

6. Stroud, C. W.: A Study of the Reaction Zone in Charring Ablators During Thermal Degradation. M.S. Thesis, Virginia Polytechnic Institute, 1965.

7. Bennett, Albert A.; Milne, William E.; and Bateman, Harry: Numerical Integration of Differential Equations. Dover Publ., Inc., 1956.

8. Dow, Marvin B.; and Swann, Robert T.: Determination of Effects of Oxidation on Performance of Charring Ablators. NASA TR R-196, 1964.

9. Dow, Marvin B.; Bush, Harold G.; and Tompkins, Stephen S.: Analysis of the Supercircular Reentry Performance of a Low-Density Phenolic-Nylon Ablator. NASA TM X-1577, 1968.

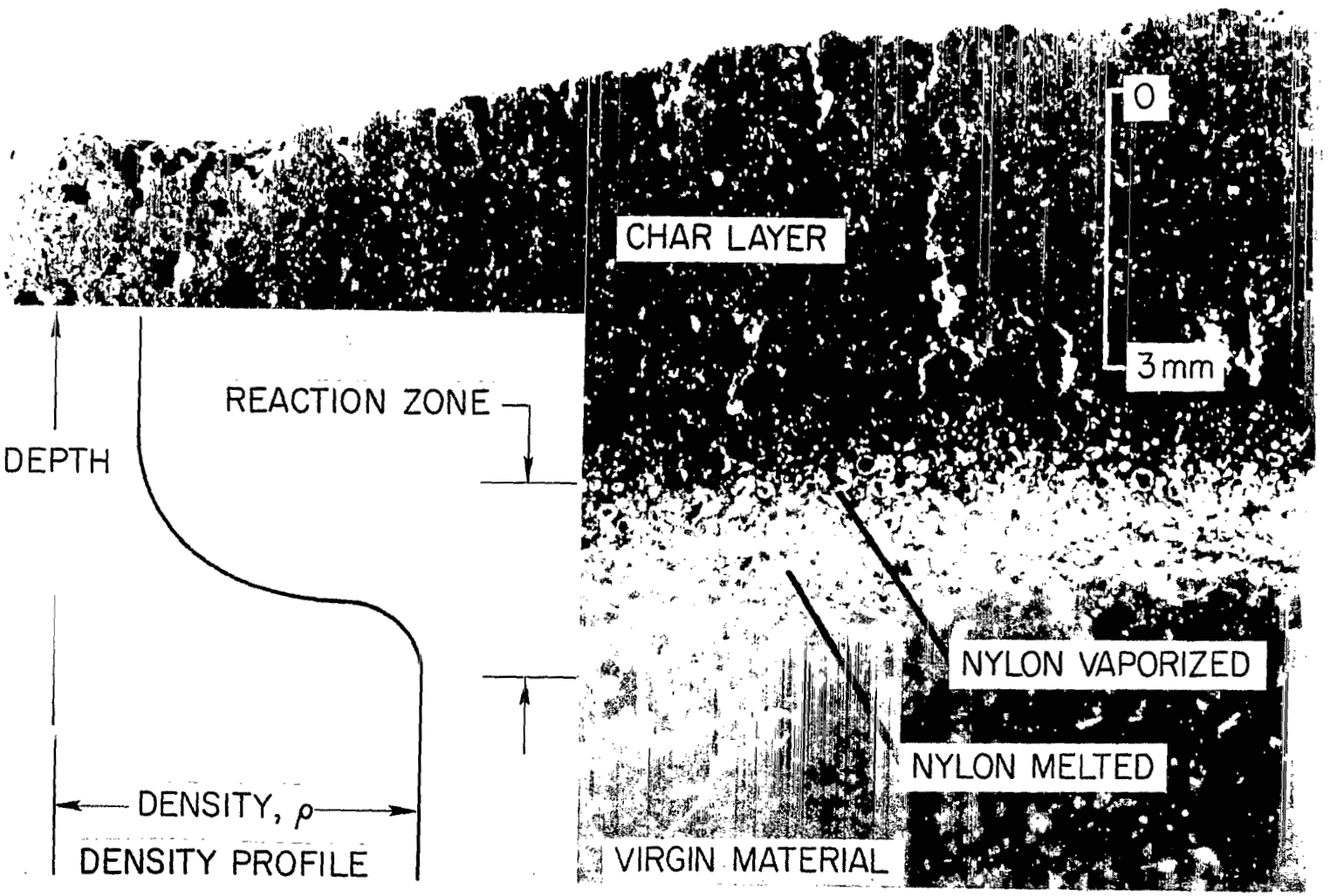

Figure 1.- Cross section of phenolic nylon after test in apparatus C of the Langley entry structures facility. L-68-5645

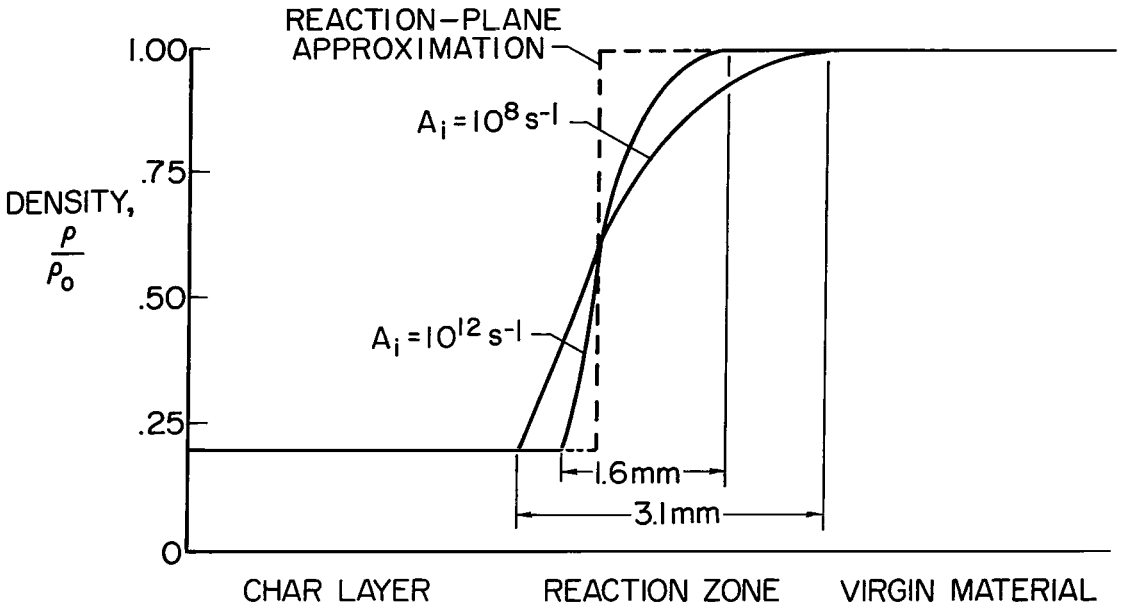

Figure 2.- Typical density profiles for first-order reactions.

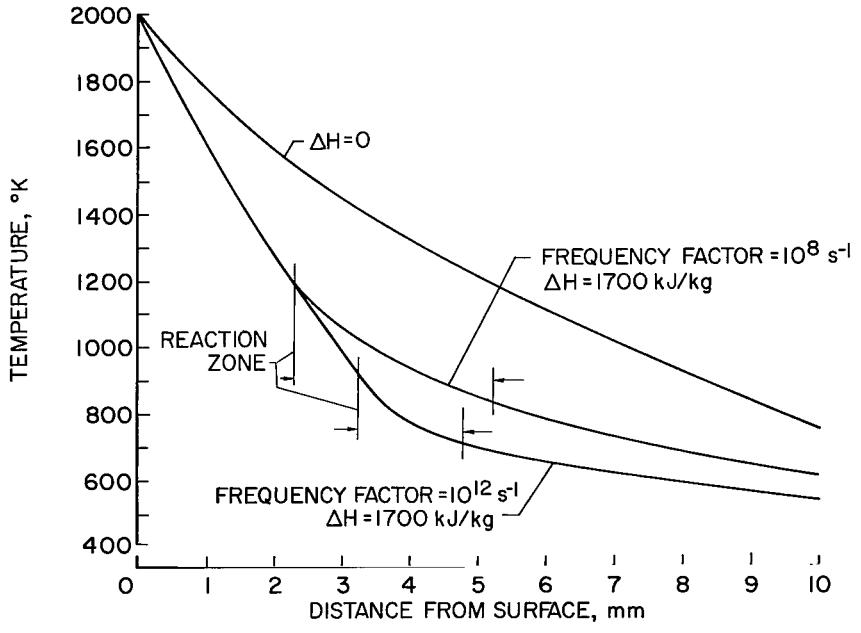

Figure 3.- Temperature profiles for first-order reactions.

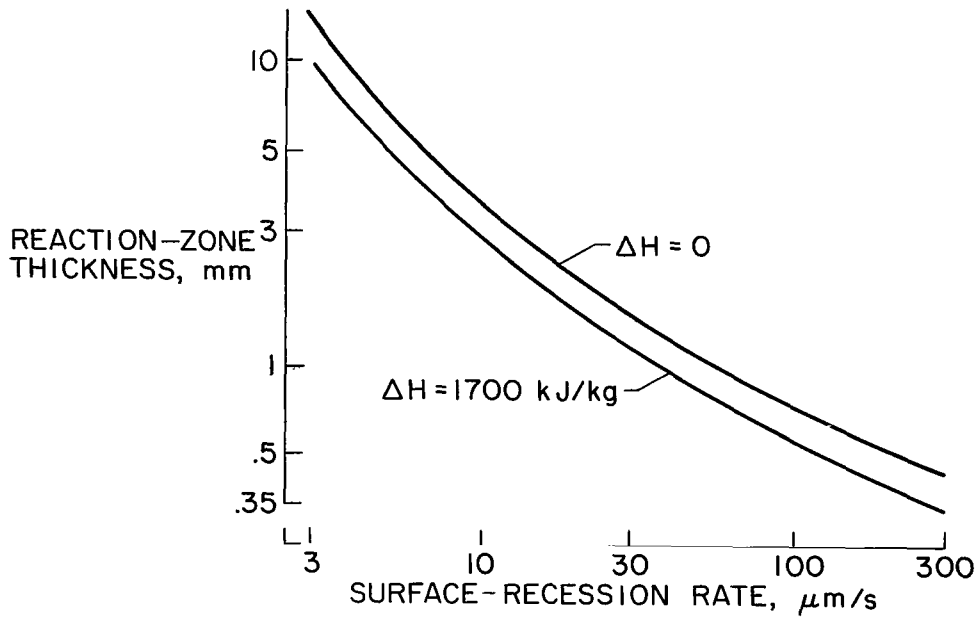

Figure 4.- Reaction-zone thickness as function of surface-recession rate. Frequency factor, 10^{12} s^{-1}.

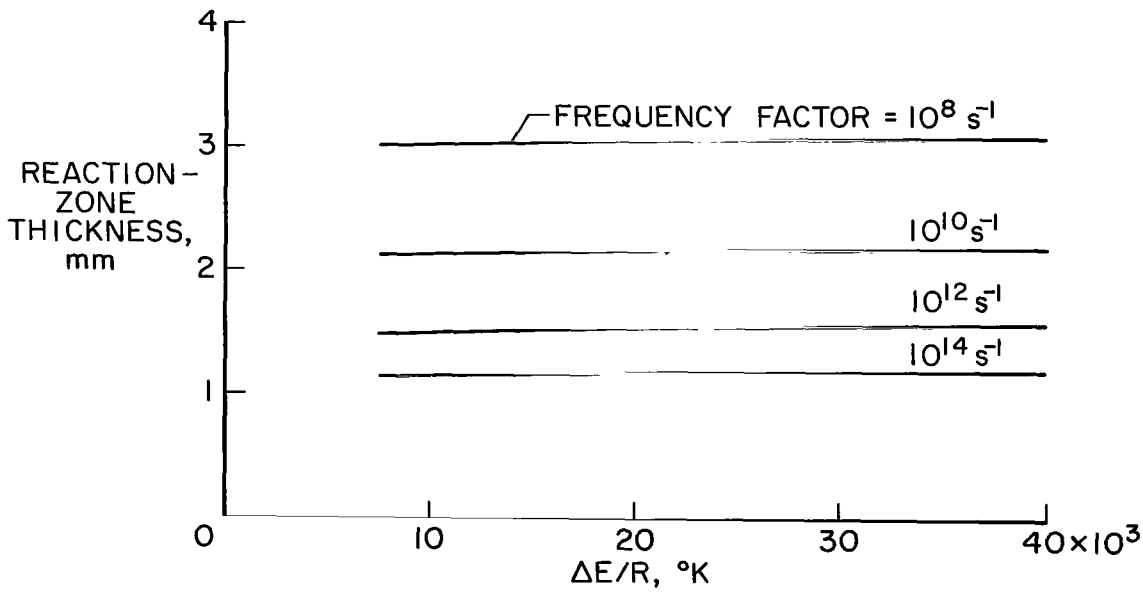

Figure 5.- Effect of activation energy on reaction-zone thickness.

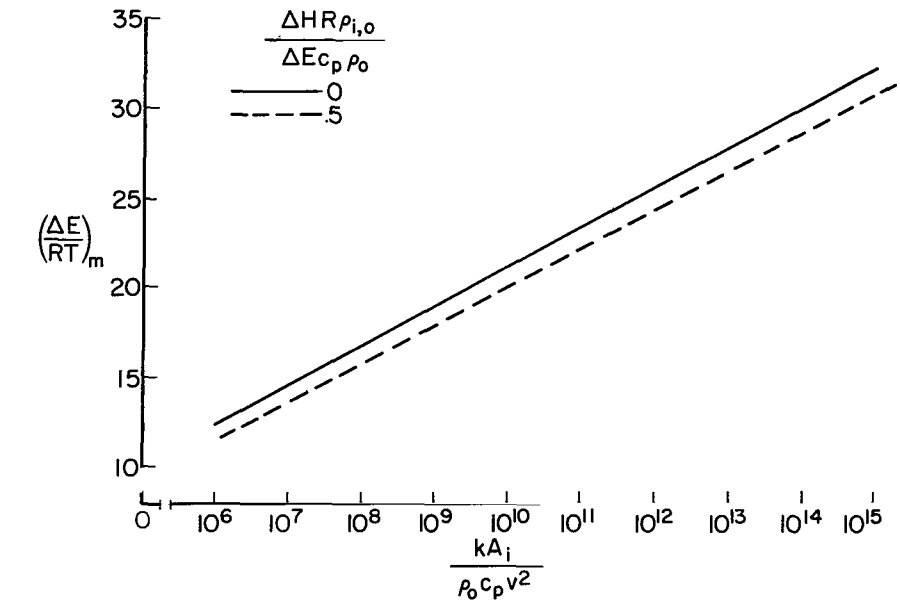

(a) Half-order reactions.

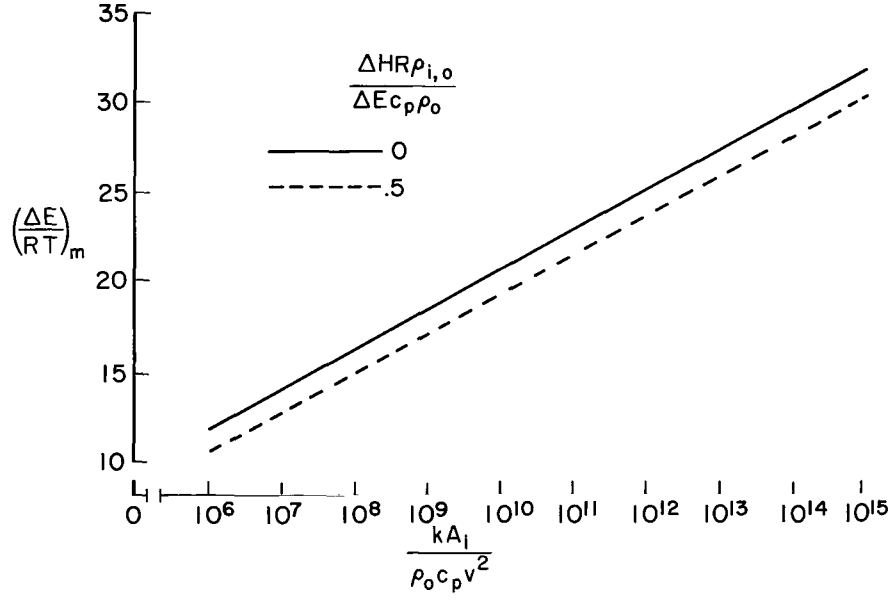

(b) First-order reactions.

Figure 6.- Reaction-zone median temperature as function of dimensionless frequency factor.

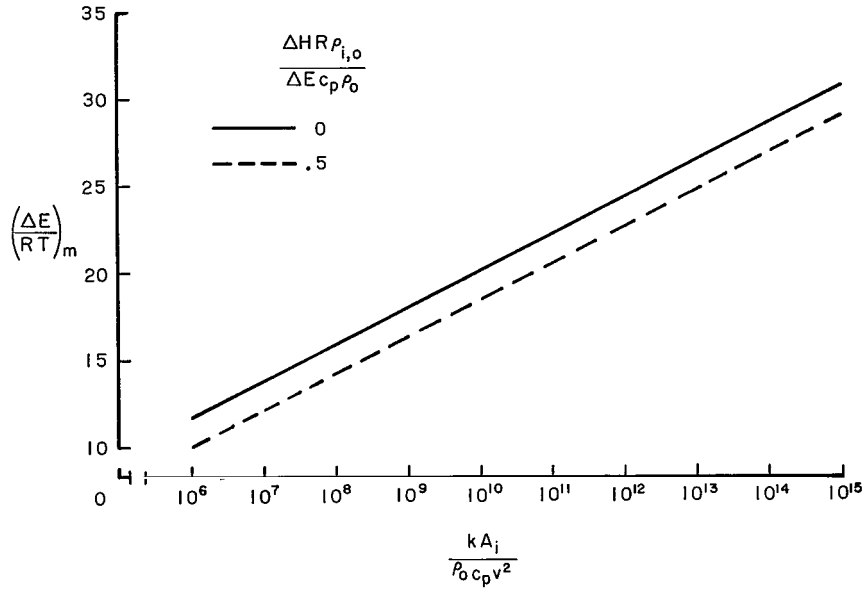

(c) Second-order reactions.

Figure 6.- Concluded.

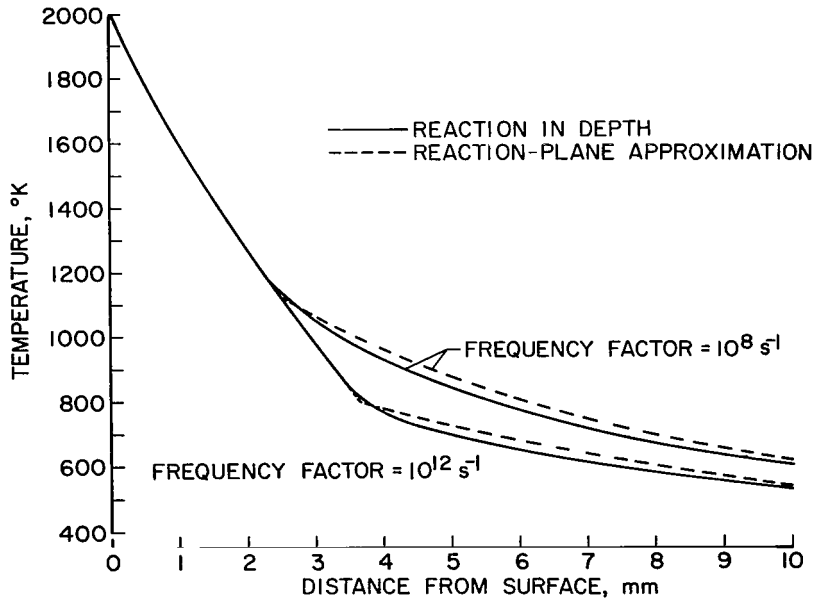

Figure 7.- Comparison of reaction-in-depth and reaction-plane analyses.

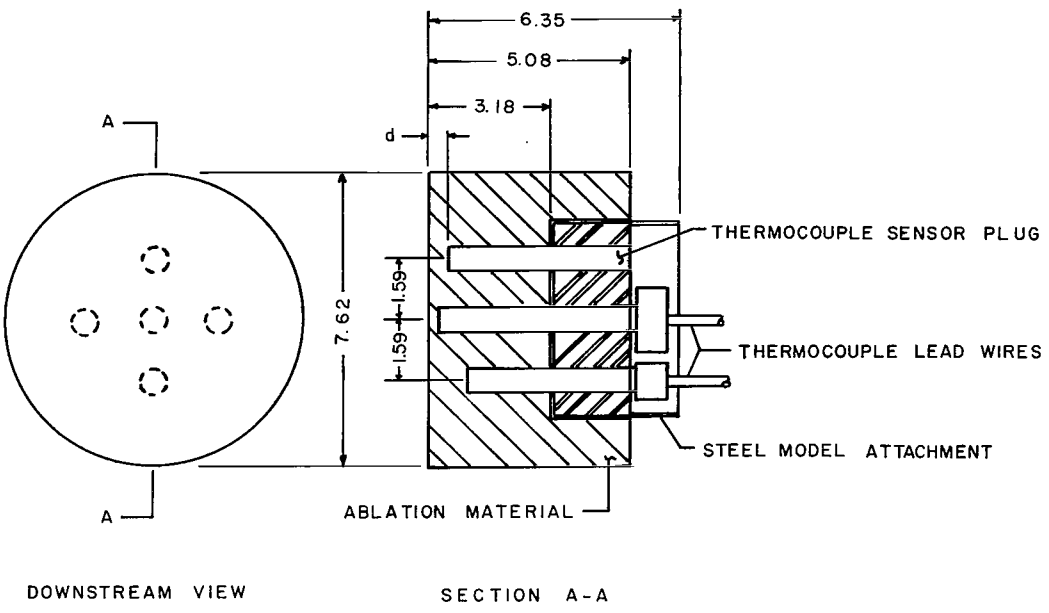

Figure 8.- Configuration of ground-test model instrumented with thermocouple sensors. (Figure taken from ref. 9.) All dimensions are in centimeters.

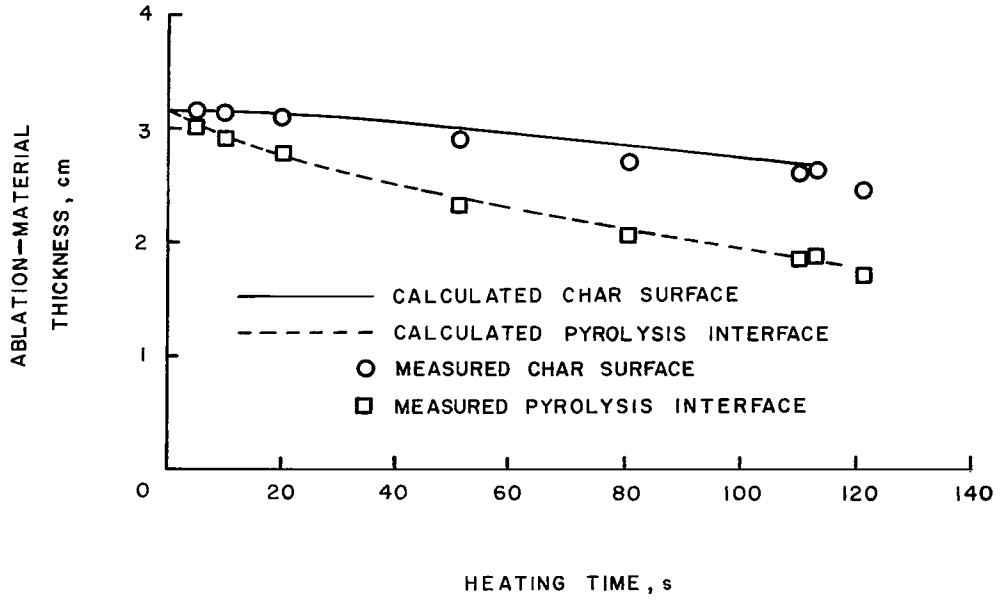

Figure 9.- Comparison of measured and calculated char-surface and pyrolysis-interface recessions. $\dot{q}_{cw}$ = 2.48 MW/m^2; h_e = 25.6 MJ/kg. (Figure taken from ref. 9.)

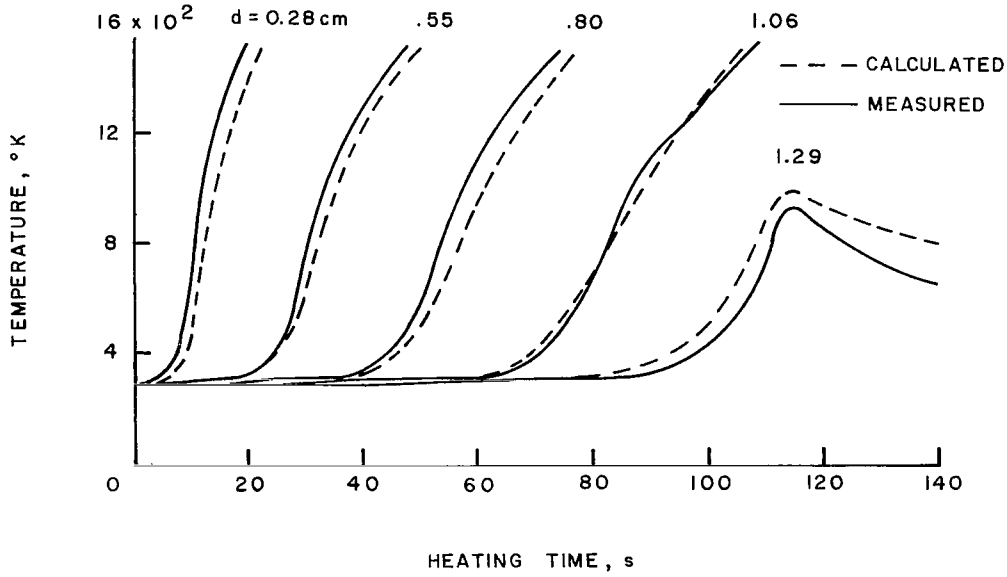

(a) Model 3.

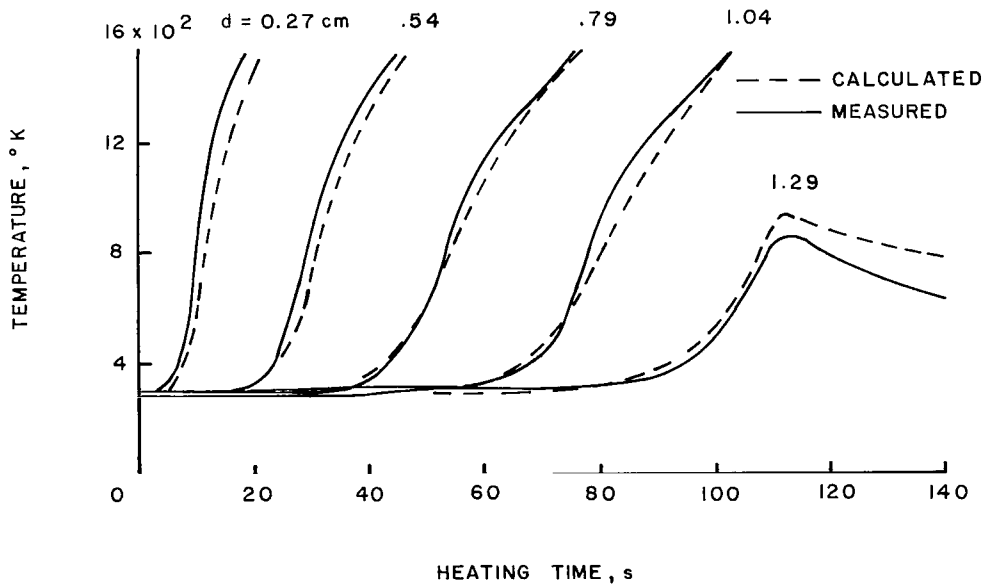

(b) Model 4.

Figure 10.- Comparison of measured and calculated ground-test-model internal temperatures. $\dot{q}_{cw}$ = 2.48 MW/m^2; h_e = 25.6 MJ/kg. (Figure taken from ref. 9.)

"The aeronautical and space activities of the United States shall be conducted so as to contribute . . . to the expansion of human knowledge of phenomena in the atmosphere and space. The Administration shall provide for the widest practicable and appropriate dissemination of information concerning its activities and the results thereof."

—NATIONAL AERONAUTICS AND SPACE ACT OF 1958

NASA SCIENTIFIC AND TECHNICAL PUBLICATIONS

TECHNICAL REPORTS: Scientific and technical information considered important, complete, and a lasting contribution to existing knowledge.

TECHNICAL NOTES: Information less broad in scope but nevertheless of importance as a contribution to existing knowledge.

TECHNICAL MEMORANDUMS: Information receiving limited distribution because of preliminary data, security classification, or other reasons.

CONTRACTOR REPORTS: Scientific and technical information generated under a NASA contract or grant and considered an important contribution to existing knowledge.

TECHNICAL TRANSLATIONS: Information published in a foreign language considered to merit NASA distribution in English.

SPECIAL PUBLICATIONS: Information derived from or of value to NASA activities. Publications include conference proceedings, monographs, data compilations, handbooks, sourcebooks, and special bibliographies.

TECHNOLOGY UTILIZATION PUBLICATIONS: Information on technology used by NASA that may be of particular interest in commercial and other non-aerospace applications. Publications include Tech Briefs, Technology Utilization Reports and Notes, and Technology Surveys.

Details on the availability of these publications may be obtained from:

SCIENTIFIC AND TECHNICAL INFORMATION DIVISION

NATIONAL AERONAUTICS AND SPACE ADMINISTRATION

Washington, D.C. 20546